Electron-impact excitation of the $n=3$ and $n=2$ states of a hydrogen atom at intermediate (14–100-eV) energies

J. Callaway
Department of Physics and Astronomy, Louisiana State University, Baton Rouge, Louisiana 70803-4001

K. Unnikrishnan
Department of Theoretical Physics, Institute of Advanced Studies, Australian National University, Canberra ACT 0200, Australia
(Received 21 June 1993)

A 17-state basis containing seven exact atomic states and ten pseudostates is employed in a calculation of cross sections for the electron-impact excitation of a hydrogen atom from the $1s$ to the $n=2$ and $n=3$ states. The incident energies range from 14 to 100 eV. The results are compared with some other recent calculations and with experiment. Improved effective (thermally averaged) collision strengths are presented for the excitation of the $n=3$ states.

PACS number(s): 34.80.Dp, 34.80.Bm

I. INTRODUCTION

Recent calculations concerning the excitation of the $2s$ and $2p$ states of hydrogen atoms at intermediate energies (roughly 13.6–100 eV) by several different methods related to close-coupling expansions have significantly increased an understanding of this old but still challenging problem [1–4]. Differential cross sections are in reasonably good agreement with experiment at selected energies [5]. There are, however, some discrepancies relating to angular correlation functions [5–10]. In this paper, we will emphasize determination of integrated cross sections as functions of energy. These are the most important quantities in applications in astrophysics and plasma physics where one requires rate coefficients that are readily obtained from the integrated cross sections. The recent calculations of the $n=2$ excitation cross sections mentioned above agree with each other within (roughly) 10%. Experimental results for these quantities for $n=2$ excitations [11,12] are, unfortunately, fairly meager and rather old.

Much less is known about the excitation of $n=3$ states in this energy range. The few calculations of the close-coupling type that have been reported differ substantially and must be considered to be of uncertain validity. There are, so far as we know, no experimental measurements of differential cross sections, a few measurements relating to orientation and alignment parameters [13,14], and a single investigation of integrated cross sections [15]. Although we report here some results for elastic scattering and $n=2$ excitations, we will focus on the $n=3$ states.

We begin with a brief summary of some previous theoretical work concerning $1s\rightarrow n=3$ transitions. Variational calculations using a 28-state basis (including all exact atomic states through $n=4$, plus 18 pseudostates) have been reported in the low-energy region, below the $n=4$ threshold [16]. A complicated structure of overlapping resonances in different partial waves has been found. There are also two shape resonances just above the $n=3$ threshold ($^3P^o$ and $^1D^e$) which were recently studied by Ho [17]. These two resonances, however, seem to have little effect on the $1s\rightarrow n=3$ excitations. Aggarwal *et al.* [18] have reported R-matrix close-coupling calculations using a basis of all 15 exact atomic states through $n=5$, covering energies from threshold up to an incident energy of 27 eV. Their results agree rather well with the variational calculations where there is overlap. Above the ionization threshold, however, their results differ quite significantly from our previous work in which a second-order optical potential was incorporated into a six-state close-coupling calculation [1]. At an incident energy of 1.96 Ry, the results of Aggarwal *et al.* [18] for $3s$ excitation are larger than those of Ref. [1] by nearly a factor of 2 for $3s$ excitation, while for $3p$, the factor is greater than 2. In the case of $3d$, the situation is not so extreme, although surprisingly, the direction is reversed: the optical potential results are larger by about 25% at this energy. It is, of course, possible that neither calculation is accurate in this energy range.

Quite recently results of an intermediate-energy R-matrix calculation for $n=1$ and $n=2$ transitions to $n=3$ were reported for a single partial wave (^1S) [19]. Although this approach is quite promising, the results now available are not yet sufficient for comparison with experiment.

The present calculation was undertaken in order to determine more accurate results for $n=3$ excitation from the ionization threshold up to 100 eV. To do this, we decided to perform close-coupling calculations employing a basis containing both exact atomic states and pseudostates. The channels associated with the pseudostates are allowed to be open, which means that the wave-function components in the pseudochannels show oscillatory asymptotic behavior. The particle flux into open pseudostate channels at energies above the ionization threshold is moderately successful in simulating ionization [20] and leads to much improved (generally smaller) values for cross sections for bound-state excitation in comparison to

a calculation employing only exact bound states in the target basis.

This paper is organized as follows. The pseudostate basis employed is described in Sec. II, which also contains a brief discussion of important features of our calculative procedures. Our results for elastic scattering and excitation of the $n=2$ and $n=3$ states are presented in Sec. III. For technical reasons associated with the extremely slow convergence of the partial-wave expansion, we defer consideration of $n=2$ to $n=3$ transitions to a subsequent paper. In Sec. IV, we combine the present results with those of Refs. [16,18] in order to obtain improved values of effective (thermally averaged) collision strengths for $1s \rightarrow n=3$ transitions.

II. CALCULATION PROCEDURES

The radial basis wave functions for target angular momentum l are expressed as a combination of orbitals as follows:

$$R_{jl}(r)=\sum_i c_{ji} r^{n_i} e^{-\zeta_i r} . \quad (1)$$

The index j denotes the state number, which may refer either to an exact atomic state or a pseudostate. The basis set is determined when the n_i and ζ_i are specified. The coefficients c_{ji} and the energies E_j are determined by diagonalization of the isolated atom Hamiltonian.

The orbital basis, defined by the chosen values of n_i and ζ_i, was chosen to meet the following objectives: (1) it had to contain the components required to generate all the exact atomic wave functions through $n=3$; (2) the exact ground-state dipole and quadrupole polarizabilities should be reproduced, and functions should be included in order to enable a reasonable description of short-range correlations. In addition, because we were seriously concerned about the correctness of our previously reported results for $3d$ excitation, we thought it important to include the exact $4f$ state with which the $3d$ interacts strongly. The parameters chosen, and the energies E_j of the states are listed in Table I.

There are $8s$, $5p$, $3d$, and $1f$ states in the basis (8-5-3-1 set). Inspection of the energies in Table I shows that the set contains a fair approximation to the $4s$ and $4p$ states, and eight states with energies in the continuum. We expect this set to be adequate above the ionization threshold well up into the continuum, hopefully up to around 100 eV. This basis set will not be a good one in the resonance region below the ionization threshold: there one requires (at least) the exact $n=4$ states and functions capable of describing long-range correlations, as is the case for the 11-9-5-2-1 basis set used in Ref. [16]. Hence we confine our presentation of results in the next section to energies above the ionization threshold.

We employed two methods in the solution of the coupled integro-differential equations. For small values of the total angular momentum ($L \leq 3$), we employed the algebraic variational method [21]. For larger values of L, we employed a linear algebraic integral-equation approach [22]. The variational method appears to be superior in terms of its ability to handle closed channels, but is limited to small angular momentum; the integral-equation approach has no obvious limitations in regard to angular momentum, but requires substantial computer memory when there are many channels. A radial grid of 253 points was employed. For the energies considered, there were at most 30 open channels. Our choice of the number of basis functions discussed above was constrained by available computer-memory requirements.

TABLE I. Parameters and energies of the 8-5-3-1 pseudostate set.

i	n_i	ζ_i	E_i (Ry)
		$l=0$	
1	0	1.0000	−1.0000
2	0	0.5000	−0.2500
3	1	0.5000	−0.1111
4	0	0.3333	−0.0587
5	1	0.3333	+0.0270
6	2	0.3333	0.3306
7	1	1.0	1.5347
8	0	1.5	9.5975
		$l=1$	
1	1	1.0000	−0.2500
2	1	0.5000	−0.1111
3	1	0.3333	−0.0388
4	2	0.3333	+0.2770
5	2	1.0000	2.1179
		$l=2$	
1	2	1.0000	−0.1111
2	3	1.0000	+0.1072
3	2	0.3333	1.3183
		$l=3$	
1	3	0.2500	−0.0625

The integral equation calculations were made in an angular momentum range $4 \leq L \leq L_m$, where L_m increased with energy from $L_m=9$ at $k^2=1.00$ to $L_m=23$ at $k^2=4.0$, 5.0, and $L_m=35$ at $k^2=7.35$. Cross sections were extrapolated to $L=\infty$ under the assumption of a geometric series. However, L_m is sufficiently large so that the extrapolated contribution, which only has to be considered for p and d states, is small. For example, the extrapolated contribution ($L > L_m$) to the $3p$ cross section is less than 1% at $k^2=4.0$ and about 1.6% at $k^2=7.35$. Even if the error in extrapolation is as large as 30%, which we believe to be unlikely, the error in the final results would be less than 0.5% at the highest energy, and much less in other cases.

The use of a small set of discrete pseudostates to represent the continuum leads to strongly energy-dependent but unphysical structure ("pseudoresonances") near the pseudostate thresholds. This has to be removed by some averaging procedure. We employed a method, previously described in Ref. [23], in which a least-squares fit is made to the complex transition amplitudes for a given L and S with a low-order polynomial in energy. This averaging procedure was applied for $L \leq 5$. We

found that the pseudothreshold structure was small enough to be neglected for $L \geq 6$. Further, we see from Table I that there are no pseudothresholds in the range of 45–100 eV. Our results for incident energies $k^2=4.0$, 5.0, and 7.35 did not require this averaging.

The averaging process requires calculation on a relatively closely spaced grid of energies on which the pseudothreshold structure is resolved. We used 31 points, ranging from $k^2=0.98$ to $k^2=3.5$. Calculations were performed for $L \leq 5$ at each of these energies plus the three higher-energy points mentioned above. The extension to higher L is quite time consuming. This was carried out ($6 \leq L \leq L_m$) for 11 energies ($k^2=1.00$, 1.21, 1.44, 1.80, 2.20, 2.60, 3.00, 3.50, 4.00, 5.00, and 7.35). As the sums of high-L partial cross sections were smooth functions of energy, we simply used Lagrangian interpolation to determine the high-L contribution at the remainder of the energies considered. Although this procedure is less than optimal, we believe that the resulting uncertainties are much smaller than those introduced by the necessary process of averaging over the pseudothresholds.

III. RESULTS: CROSS SECTIONS

Our results for elastic scattering, $1s \rightarrow n=2$, $1s \rightarrow n=3$ transitions, and the total cross section are given in Table II.

We consider elastic scattering first. Our cross sections are shown graphically in Fig. 1. We show for comparison results of the "intermediate-energy R-matrix" calculation of Scott *et al.* [2] (open circles) and the Sturmian-basis close-coupling calculation of Bray and Stelbovics [4] (open squares). The agreement is reasonably good. The total cross section is also shown in Fig. 1. We are particularly encouraged by the rather good agreement between our results and those of Ref. [4], as those authors argue that their results are converged with respect to the number of basis functions. It appears that a modest number of carefully chosen pseudostates can give results quite comparable in quality to a much larger but unselective basis. We are not aware of any experimental measurements of these fundamental cross sections in this energy range.

TABLE II. Integrated cross sections (units πa_0^2) for elastic scattering, $1s \rightarrow n=2$, $1s \rightarrow n=3$ transitions and the total cross section.

	Cross section						
E (Ry)	1s-1s	1s-2s	1s-2p	1s-3s	1s-3p	1s-3d	1s-tl
1.05	4.931	0.140	0.433	0.031	0.062	0.036	5.827
1.10	4.682	0.130	0.453	0.027	0.061	0.037	5.632
1.15	4.455	0.122	0.476	0.025	0.066	0.038	5.457
1.21	4.206	0.116	0.504	0.025	0.076	0.040	5.267
1.25	4.053	0.112	0.523	0.025	0.083	0.041	5.149
1.30	3.875	0.108	0.545	0.025	0.091	0.041	5.015
1.35	3.708	0.105	0.565	0.025	0.098	0.041	4.892
1.44	3.439	0.101	0.597	0.024	0.109	0.040	4.695
1.50	3.276	0.098	0.615	0.023	0.113	0.039	4.580
1.60	3.033	0.094	0.639	0.022	0.118	0.036	4.411
1.69	2.838	0.090	0.656	0.020	0.119	0.035	4.279
1.80	2.627	0.086	0.673	0.017	0.120	0.033	4.138
1.90	2.457	0.084	0.685	0.016	0.119	0.031	4.026
2.00	2.305	0.081	0.695	0.015	0.118	0.030	3.925
2.10	2.168	0.079	0.704	0.014	0.117	0.029	3.832
2.20	2.044	0.078	0.712	0.013	0.116	0.029	3.745
2.30	1.931	0.076	0.719	0.013	0.116	0.028	3.663
2.40	1.829	0.075	0.726	0.013	0.116	0.027	3.584
2.50	1.735	0.074	0.733	0.013	0.117	0.027	3.507
2.60	1.649	0.074	0.739	0.013	0.117	0.026	3.434
2.70	1.570	0.073	0.745	0.013	0.118	0.025	3.364
2.80	1.497	0.072	0.750	0.013	0.119	0.024	3.296
2.90	1.430	0.071	0.754	0.013	0.120	0.024	3.234
3.00	1.369	0.070	0.758	0.013	0.121	0.023	3.174
3.10	1.313	0.069	0.760	0.012	0.122	0.022	3.119
3.20	1.262	0.068	0.762	0.012	0.123	0.022	3.068
3.30	1.214	0.067	0.762	0.012	0.124	0.022	3.022
3.40	1.171	0.065	0.762	0.011	0.124	0.021	2.978
3.50	1.131	0.064	0.761	0.011	0.125	0.022	2.938
4.00	0.950	0.062	0.748	0.011	0.121	0.019	2.746
5.00	0.715	0.054	0.721	0.0102	0.116	0.016	2.422
7.35	0.445	0.041	0.637	0.0081	0.103	0.011	1.956

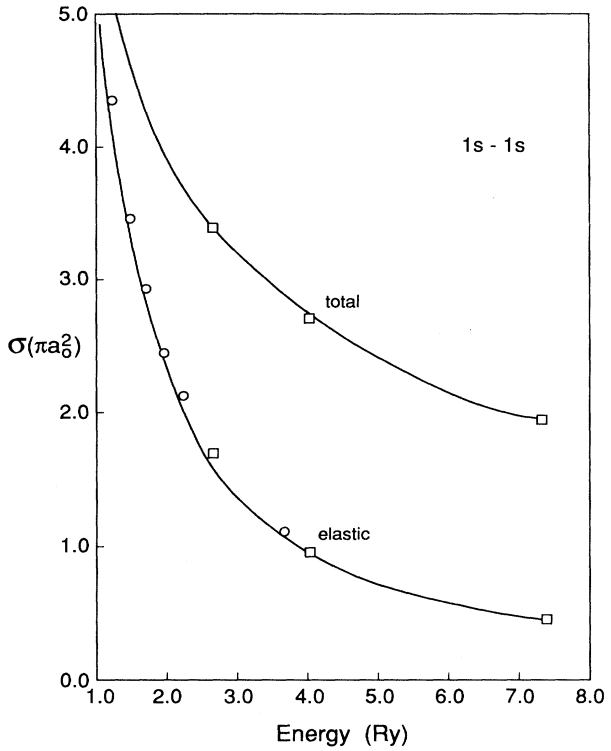

FIG. 1. $1s$ elastic scattering and total cross sections (units πa_0^2). Solid curves, our results; open circles, results of Ref. [2]; squares, results of Ref. [4].

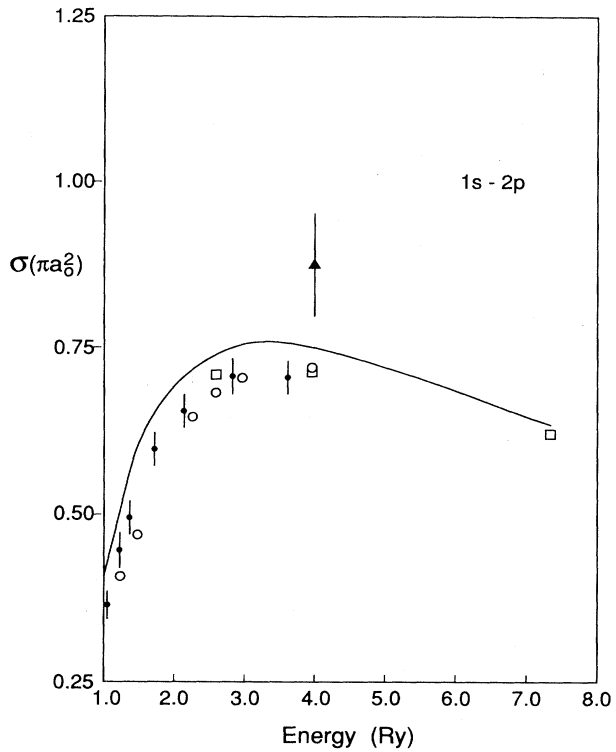

FIG. 3. Similar to Fig. 2 but for $1s \rightarrow 2p$ excitation. The solid triangle with large error bars is an absolute measurement reported in Ref. [5].

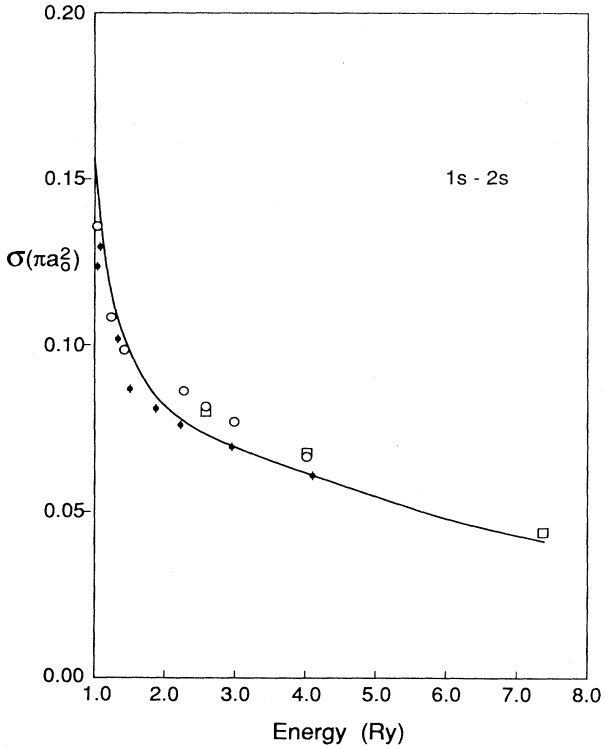

FIG. 2. $1s \rightarrow 2s$ excitation cross section (units πa_0^2). Solid curve, our results; open circles, results of Ref. [2]; squares, results of Ref. [4]. Experimental points with error bars were obtained as described in the text.

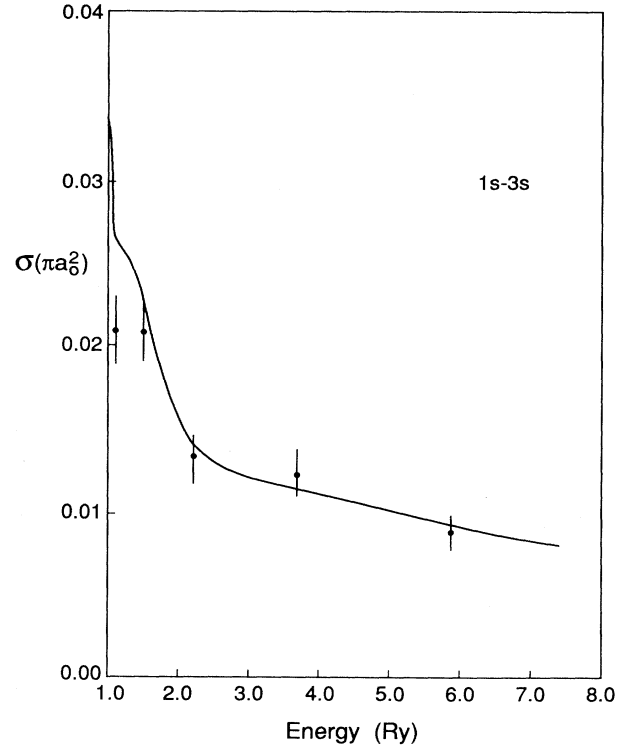

FIG. 4. $1s \rightarrow 3s$ excitation cross section (units πa_0^2). The experimental points with error bars were obtained from graphical data in Ref. [15]. The curve is based on a smooth fit to the data of Table II.

Our results for $1s \rightarrow 2s$ and $1s \rightarrow 2p$ transitions are shown in Figs. 2 and 3, respectively. They are compared with the theoretical results of Scott *et al.* [2] and Bray and Stelbovics [4] as above. We have also attempted to include experimental results. This is, however, not simple. The basic experimental observations reported in Refs. [11,12] involve the detection of Lyman-α photons emitted when the excited hydrogen atoms decay to their ground state. In the case of $2p$ excitation, the decay is almost immediate, but the much longer lived $2s$ state must be quenched through the application of an external electric field. There are two critical problems: (1) normalization of the cross sections, and (2) correction for cascade from higher states into the $n=2$ levels. Significant uncertainties are involved. We have not attempted to make an independent analysis of these effects. Instead, we have simply utilized the results of the analysis of the experimental measurements contained in Ref. [2], and we have reproduced in our Figs. 2 and 3 the values given in the similar figures in Ref. [2]. The agreement between our results and the analyzed experimental data is rather good for the $2s$, but our results are consistently higher than those data points for the $2p$. In the case of the $2p$ excitation, there is a single point at 54.4 eV from an absolute measurement of Williams [5]. This value does not agree well either with the theories or with the other experimental results as interpreted in Ref. [2]. Clearly, further experimental investigation is required.

We now consider the results for $3s$, $3p$, and $3d$ excitation, which are shown in Figs. 4, 5, and 6. Our results as shown here are based on a smooth fit (as described below in Sec. IV) to the data of Table II. The experimental points with error bars were obtained from graphical data in Ref. [15]. We think the agreement is reasonably good, perhaps surprisingly so.

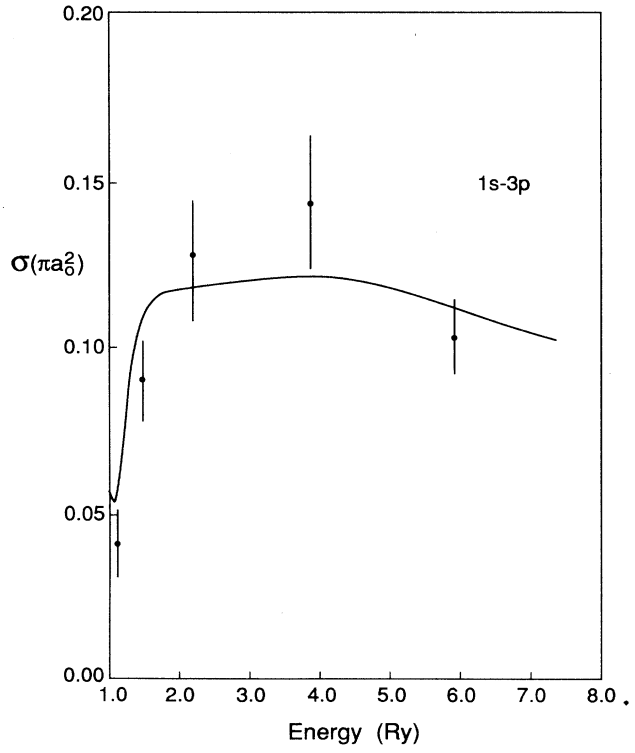

FIG. 5. Similar to Fig. 4 for $1s$-$3p$ excitations.

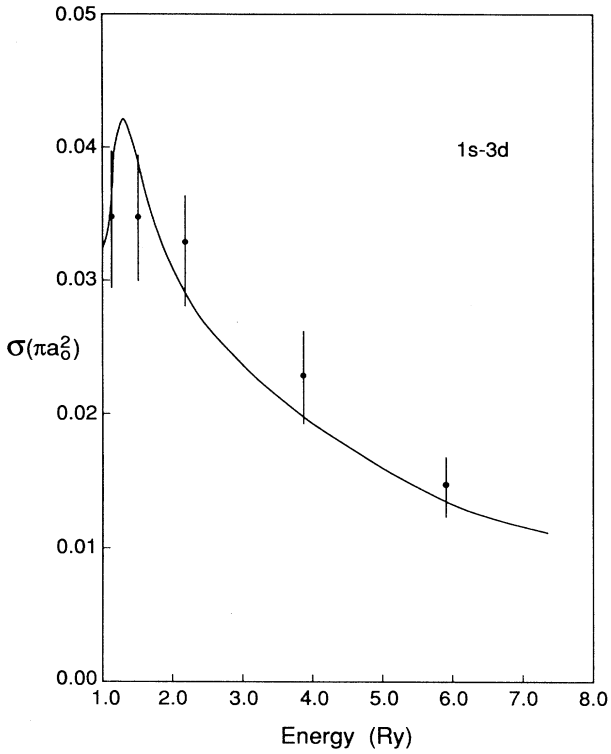

FIG. 6. Similar to Fig. 4 for $1s$-$3d$ excitation.

The figures do not show previous theoretical results, as many would be off scale. We confirm the suspected inadequacy of a basis consisting entirely of bound atomic states at energies above the ionization threshold. At $k^2=1.44$ the results of Aggarwal *et al.* [18] are larger than the present ones by a factor of 2.5 for $2s$ excitation and 2.1 for $3p$ excitation. For the $3d$ excitation, the discrepancy is much smaller ($\sim 20\%$) but in the same direction. We would like to emphasize that we do not criticize the results of Ref. [18] below the ionization threshold. Moreover we think that the present results are a considerable improvement over our previous optical potential calculations [1]. The differences are not at all so large as we found in regard to those of Ref. [18] and are not easy to describe simply. Quantitatively most differences are in the range $\pm 10\%$ to $\pm 30\%$ (both signs occur) in contrast to factors of 2.

IV. EFFECTIVE COLLISION STRENGTHS

The effective collision strength for a transition i-f, denoted here γ_{if}, is a thermal average of the cross section over a Maxwell distribution of electron velocities. It is dimensionless, but rather simply related to the excitation rate coefficient. Specifically if σ_{if} is the cross section,

$$\gamma_{if}=\int_0^\infty \Omega_{if} e^{-E_f/k_B T} d(E_f/k_B T) , \tag{2}$$

where E_f is the kinetic energy of the outgoing electron, T is the plasma temperature, k_B is Boltzmann's constant, and

$$\Omega_{if}=g_i k_i^2 \sigma_{if}(k_i^2) , \tag{3}$$

with k_i^2 being the incident electron energy (in Ry). Finally g_i is the degeneracy of the initial state including spin (thus $g_{1s}=2$).

The effective collision strengths for $1s \rightarrow n=2$ excitations of hydrogen atoms are given adequately from previous work and are not discussed here. The interested reader will find a review of calculations of effective collision strengths for neutral hydrogen and hydrogenic ions, considering work up to March 1992, in Ref. [24]. Since the present results for $1s \rightarrow n=3$ transitions should be a significant improvement, we have repeated the calculations of these effective collision strengths.

In order to do this, we first made least-squares fits to the quantity Ω_{if} of Eq. (3) with data from Table II, using a functional form suggested by the Born approximation

$$\Omega_{if}=\sum_{j=0}^{n} a_j x^{-j}+a_{n+1} \ln x , \tag{4}$$

where $x=k_i^2/\Delta E$, and ΔE is the excitation energy, $\frac{8}{9}$ Ry in the present case. The quantity a_{n+1} vanishes for transitions to the $3s$ and $3d$ states. We took $n=6$ for $3s$, $n=5$ for $3p$, and $n=7$ for $3d$. The resulting fits were used to generate the smooth curves of the cross sections shown in Figs. 4, 5, and 6.

The evaluation of the integral in Eq. (2) requires cross sections at lower energies than those considered in the calculations described in Secs. II and III. We used the variational results of Ref. [16] for energies from the $n=3$ threshold at 0.8889 Ry up to $k^2=0.931$ Ry. The results of Aggarwal *et al.* [18] were used in the range $0.931<k^2<1.00$. In this way, cross sections are used that are the best available in the resonance region. The final effective collision strengths are listed in Table III, and are shown graphically in Figs. 7–9. Results from Ref. [18] are shown for comparison. At low temperatures, the differences between the results are in the range of 10–15%, but are much larger for temperatures greater than 0.1 Ry. This is obviously the result of the overestimate of the excitation cross sections above the ionization threshold in Ref. [18]. The agreement with the effective collision strengths recommended in Ref. [24] is much closer, but we think the present values are preferable.

TABLE III. Effective collision strengths.

	Collision strength		
$k_B T$ (Ry)	$1s$-$3s$	$1s$-$3p$	$1s$-$3d$
0.01	0.0506	0.0969	0.0486
0.02	0.0567	0.1039	0.0542
0.03	0.0604	0.1081	0.0573
0.04	0.0624	0.1107	0.0593
0.05	0.0635	0.1127	0.0608
0.06	0.0641	0.1146	0.0620
0.07	0.0645	0.1165	0.0633
0.08	0.0646	0.1186	0.0645
0.09	0.0647	0.1209	0.0656
0.10	0.0647	0.1234	0.0668
0.15	0.0646	0.1386	0.0724
0.20	0.0645	0.1562	0.0772
0.25	0.0645	0.1743	0.0814
0.30	0.0645	0.1922	0.0849
0.35	0.0645	0.2098	0.0880
0.40	0.0645	0.2270	0.0907
0.45	0.0646	0.2436	0.0932
0.50	0.0647	0.2598	0.0954
0.60	0.0650	0.2912	0.0992
0.70	0.0654	0.3211	0.1025
0.80	0.0659	0.3497	0.1053
0.90	0.0665	0.3770	0.1078
1.00	0.0671	0.4028	0.1100

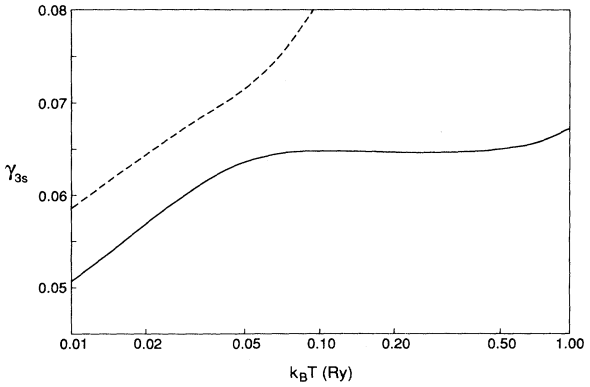

FIG. 7. Dimensionless effective collision strength for $1s$-$3s$ transitions. Solid curve, present results; dashed curve, results of Ref. [18].

A four-term empirical polynomial fit to the effective collision strengths

$$\gamma=\sum_{i=0}^{3} b_i T^i \tag{5}$$

(where T is the temperature in Ry) gives agreement to 3% (often better) for $T>0.02$ Ry. The coefficients are given in Table IV.

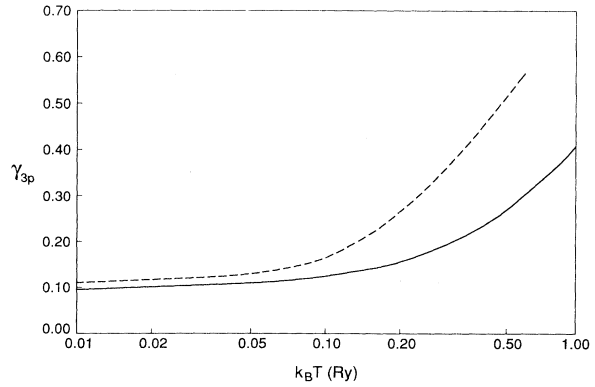

FIG. 8. Similar to Fig. 7, but for $1s$-$3p$.

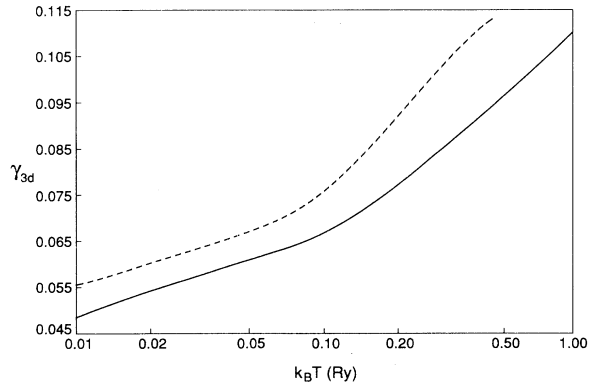

FIG. 9. Similar to Fig. 7, but for $1s$-$3d$.

V. SUMMARY

We have calculated integrated cross sections for elastic scattering, $1s \rightarrow n=2$, $1s \rightarrow n=3$ transitions, and the total cross section for electron impact on neutral hydrogen atoms for incident energies from 14 to 100 eV. The calculations are of the close-coupling type, and employ a basis containing seven exact atomic states ($1s$, $2s$, $3s$, $2p$, $3p$, $3d$, and $4f$) plus ten pseudostates ($5s$-like, $3p$-like, and $2d$-like). Pseudothreshold structure in the continuum was removed by a fitting process. The results for the $1s \rightarrow n=3$ transitions, which have not been the subject of intensive study previously, are significantly different from theoretical results in the recent literature, and are in reasonably good agreement with the one reported set of experimental measurements. In the other cases studied, $n=2$ excitations, elastic and total cross sections, the results are in fairly good though not perfect agreement with other calculations and with the relatively meager experimental results. In general, one can conclude that with a modest set of carefully chosen pseudostates, one can obtain cross sections of accuracy quite comparable to that found using other, much larger, discrete basis sets. The present results for excitation of the $n=3$ states are combined with previously published results at lower energies to generate effective (thermally averaged) collision strengths.

TABLE IV. Coefficients b_i appearing in the empirical fit to the collision strengths, Eq. (5).

	b_i		
i	$3s$	$3p$	$3d$
0	0.0588	0.0967	0.0520
1	0.0512	0.2807	0.1600
2	−0.1134	0.1483	−0.1884
3	0.0722	−0.1251	0.0875

ACKNOWLEDGMENT

This work was supported in part by the National Science Foundation under Grant No. 91-22117.

[1] J. Callaway, K. Unnikrishnan, and D. H. Oza, Phys. Rev. A **36**, 2576 (1987).
[2] M. P. Scott, T. T. Scholz, H. K. J. Walters, and P. G. Burke, J. Phys. B **22**, 3055 (1989).
[3] I. Bray, D. A. Konovalov, and I. E. McCarthy, Phys. Rev. A **44**, 5586 (1991).
[4] I. Bray and A. T. Stelbovics, Phys. Rev. A **46**, 6995 (1992).
[5] J. F. Williams, J. Phys. B **14**, 1197 (1981).
[6] S. T. Hood, E. Weigold, and A. J. Dixon, J. Phys. B **12**, 631 (1979).
[7] E. Weigold, L. Frost, and K. J. Nygaard, Phys. Rev. A **21**, 1950 (1980).
[8] J. Slevin, M. Eminyan, J. M. Woolsey, G. Vassilev, and H. Q. Porter, J. Phys. B **13**, L341 (1980).
[9] J. Slevin, M. Eminyan, J. M. Woolsey, G. Vassilev, H. Q. Porter, C. G. Back, and S. Watkin, Phys. Rev. A **26**, 1344 (1982).
[10] J. F. Williams, Aust. J. Phys. **39**, 621 (1986).
[11] R. L. Long, D. M. Cox, and S. J. Smith, J. Res. Natl. Bur. Stand. Sec. A **72**, 521 (1968).
[12] W. E. Kauppila, W. R. Ott, and W. L. Fite, Phys. Rev. A **1**, 1099 (1970).
[13] S. Chwirot and J. Slevin, J. Phys. B **20**, 3885 (1987).
[14] D. Farrell, S. Chwirot, R. Srivastava, and J. Slevin, J. Phys. B **23**, 315 (1990).
[15] A. H. Mahan, Ph.D. thesis, University of Colorado, available from University Microfilms International, Ann Arbor, MI; A. H. Mahan, A. Gallagher, and S. J. Smith, Phys. Rev. A **13**, 156 (1976).
[16] J. Callaway, Phys. Rev. A **37**, 3692 (1988); **43**, 5175 (1991).
[17] Y. K. Ho (private communication).
[18] K. M. Aggarwal, K. A. Berrington, P. G. Burke, A. E. Kingston, and A. Pathak, J. Phys. B **24**, 1385 (1991).
[19] M. P. Scott and P. G. Burke, J. Phys. B **26**, L191 (1993).
[20] J. Callaway and D. H. Oza, Phys. Lett. **72A**, 207 (1979).
[21] J. Callaway, Phys. Rep. **45**, 89 (1978).
[22] D. H. Oza and J. Callaway, J. Comput. Phys. **68**, 89 (1987).
[23] J. Callaway, Phys. Rev. A **32**, 775 (1985).
[24] J. Callaway, At. Data Nucl. Data Tables (to be published).